Photolysis and oxidation by OH radicals of two carbonyl nitrates: 4-nitrooxy-2-butanone and 5-nitrooxy-2-pentanone

Bénédicte Picquet-Varrault[1], Ricardo Suarez-Bertoa[2], Marius Duncianu[3], Mathieu Cazaunau[1], Edouard Pangui[1], Marc David[1], Jean-François Doussin[1]

[1] LISA, UMR CNRS 7583, Université Paris-Est Créteil, Université de Paris, Institut Pierre Simon Laplace (IPSL), Créteil, France

[2] European Commission Joint Research Centre (JRC), Ispra, Italy

[3] System Analyst Interscience BV, Brussels, Belgium

Correspondence to: B. Picquet-Varrault (benedicte.picquet-varrault@lisa.u-pec.fr)

Abstract

Multifunctional organic nitrates, including carbonyl nitrates, are important species formed in NOx rich atmospheres by the degradation of VOCs. These compounds have been shown to play a key role in the transport of reactive nitrogen and consequently in the ozone budget, but also to be important components of the total organic aerosol. However, very little is known about their reactivity in both gas and condensed phases. Following a previous study we published on the gas-phase reactivity of α-nitrooxy ketones, the photolysis and the reaction with OH radicals of 4-nitrooxy-2-butanone and 5-nitrooxy-2-pentanone, respectively a β-nitrooxy ketone and a γ-nitrooxy ketone, were investigated for the first time in simulation chambers. The photolysis frequencies were directly measured in CESAM chamber which is equipped with a very realistic irradiation system. The ratios $j_{nitrate}/j_{NO2}$ were found to be $(5.9 \pm 0.9) \times 10^{-3}$ for 4-nitrooxy-2-butanone and $(3.2 \pm 0.9) \times 10^{-3}$ for 5-nitrooxy-2-pentanone under our experimental conditions. From these results, it was estimated that ambient photolysis frequencies calculated for typical tropospheric irradiation conditions corresponding to the 1st July at noon and at 40° latitude North (overhead ozone column 300, albedo 0.1) are $(6.1 \pm 0.9) \times 10^{-5}$ s^{-1} and $(3.3 \pm 0.9) \times 10^{-5}$ s^{-1} for 4-nitrooxy-2-butanone and 5-nitrooxy-2-pentanone, respectively. These results demonstrate that photolysis is a very efficient sink for these compounds with atmospheric lifetimes of few hours. They also suggest that, similarly to α-nitrooxy ketones, β-nitrooxy ketones have enhanced UV absorption cross sections and quantum yields equal or close to unity and that γ-nitrooxy ketones have lower enhancement of cross sections which can easily be explained by the larger distance between the two chromophore groups. Thanks to a product study, branching ratio between the two possible photodissociation pathways are also proposed. Rate constants for the reaction with OH radicals were found to be $(2.9 \pm 1.0) \times 10^{-12}$ cm^3 molecule^{-1} s^{-1} and $(3.3 \pm 0.9) \times 10^{-12}$ cm^3 molecule^{-1} s^{-1}, respectively. These experimental data are in good agreement with rate constants estimated by the SAR of Kwok and Atkinson (1995) when using the parametrization proposed by Suarez-Bertoa et al. (2012) for carbonyl nitrates. Comparison with photolysis rates suggests that OH-

initiated oxidation of carbonyl nitrates is a less efficient sink than photodissociation but is not

38 negligible in polluted area.

1 Introduction

40 Organic nitrates play an important role as sinks or temporary reservoirs of NOx, as well as on ozone production in the atmosphere (Perring et al., 2013; Perring et al., 2010; Ito et al., 2007). They are formed by the degradation

42 of VOCs in presence of NOx through two main processes: i) the reaction of peroxy radical, produced by the oxidation of VOCs, with NO. The major pathway is generally the reaction (1a) that leads to NO_2 formation. The

44 reaction (1b) is a minor channel but it becomes gradually more important with increasing peroxy radical carbon chain length (Atkinson and Arey, 2003; Finlayson-Pitts and Pitts, 2000).

46 $\quad$ $RO_2 + NO \rightarrow RO + NO_2$ $\qquad$ (1a)

$\quad$ $RO_2 + NO \rightarrow RONO_2$ $\qquad$ (1b)

48 ii) The reaction of unsaturated VOCs with NO_3 radical, which proceeds mainly by addition of the nitrate radical on the double bond to produce nitro-alkyl radicals that can evolve into organic nitrates.

50 Among the organic nitrates, a variety of multifunctional species such as hydroxy-nitrates, carbonyl-nitrates and dinitrates are formed. The formed species have been shown to significantly contribute to the nitrogen budget in

52 both rural and urban areas (Perring et al. 2013). Beaver et al. (2012) have observed that carbonyl nitrates, formed as second generation nitrates from isoprene, are an important fraction of the total organic nitrates observed over

54 Sierra Nevada in summer. These observations are supported by several studies that investigated the photooxidation of isoprene in simulation chambers (Paulot et al., 2009, Müller et al., 2014). These

56 multifunctional organic nitrates are also semi-/non-volatile and highly soluble species and are thus capable of partitioning into the atmospheric condensed phases (droplets, aerosols). Numerous field observations of the

58 chemical composition of atmospheric particles have shown that organic nitrates represent a significant fraction (up to 75% in mass) of the total organic aerosol (OA) demonstrating that these species are important components

60 of total OA (Ng et al., 2017).

Several modeling studies have also confirmed that multifunctional organic nitrates, in particular isoprene

62 nitrates, play a key role in the transport of reactive nitrogen and consequently in the formation of ozone and other secondary pollutants at the regional and global scales (Horowitz et al., 2007; Mao et al., 2013; Squire et al.,

64 2015). In particular, Mao et al. (2013) have performed simulations based on data from the ICARTT aircraft campaign across the eastern U.S. in 2004. They have shown that organic nitrates, which are mainly composed of

66 secondary organic nitrates, including a large fraction of carbonyl nitrates, provide an important pathway for exporting NOx from the U.S.'s boundary layer, even exceeding the export of peroxy acyl nitrates (PANs).

68 However, these modeling studies also point out the need for additional experimental data to better describe the sinks in both gas and condensed phases of multifunctional organic nitrates in models.

70 Recent experimental studies have revealed that hydrolysis in aerosol phase may be a very efficient sink of organic nitrates in the atmosphere (Bean and Hildebrand Ruiz, 2015; Rindelaub et al., 2015). These studies also

72 suggest that the rate of these reactions strongly depends on the organic nitrate chemical structure and that

additional work is needed to better understand these processes. In the gas-phase, photolysis and reaction with OH radical are expected to dominate the fate of organic nitrates (Roberts et al., 1990; Turberg et al., 1990). In a previous study, we have measured the photolysis frequencies and the rate constants for the OH-oxidation of 3 carbonyl nitrates (α-nitrooxyacetone, 3-nitrooxy-2-butanone, and 3-methyl-3-nitrooxy-2-butanone) and we have shown that photolysis is the dominant sink for these compounds (Suarez-Bertoa et al., 2012). By comparison with absorption cross sections provided by Barnes et al. (1993), Müller et al. (2014) suggested i) that the α-nitrooxy ketones have enhanced absorption cross sections, due to the interaction between the –C=O and the -ONO$_2$ chromophore groups and ii) that the photolysis quantum yield is close to unity and O–NO$_2$ dissociation is the likely major channel. They also showed that this enhancement was larger at the higher wavelengths, where the absorption by the nitrate chromophore is very small. Therefore, they concluded that the absorption by the carbonyl chromophore was the one enhanced due to the neighbouring nitrate group.

These results are significant as they demonstrate that photolysis frequencies of these multifunctional species cannot be calculated as the sum of the monofunctional species (ketone + alkyl nitrate) ones. However, only α-nitrooxy ketones were studied which leaves open the question of the persistence of the enhancement effect when the distance between the two functional groups increases. More recently, Xiong et al. (2016) have studied the atmospheric degradation (photolysis, OH-oxidation and ozonolysis) of *trans*-2-methyl-4-nitrooxy-2-buten-1-al (also called 4,1-isoprene nitrooxy enal) in order to better assess – as a model compound - the reactivity of carbonyl nitrates formed by the NO$_3$-initiated oxidation of isoprene. This compound has a conjugated chromophore –C=C-C=O in β position of the nitrate group. The authors measured the absorption cross sections of the nitroxy enal and compared them to those for the monofunctional species, i.e. methacrolein and isopropyl nitrate. They concluded that molecules containing β-nitrooxy ketones functionalities have also enhanced UV absorption cross sections. They also studied the kinetic and mechanisms for the oxidation of the nitroxy enal by OH and O$_3$. They conclude that photolysis and reaction with OH are thus the two main loss processes of *trans*-2-methyl-4-nitrooxy-2-buten-1-al, leading to a tropospheric lifetime of less than 1 h.

Given the large contribution of the carbonyl nitrates to the organic nitrate pool and the importance of their photochemistry for the NOx budget, we present a study that aims at providing new experimental data on the gas-phase reactivity of these compounds. The study also seeks to disclose how photolysis and reaction with OH radical of carbonyl nitrates are affected by modifying their carbon chain length and the position of the two functional groups present in their molecular structure. Here, we provide the first photolysis frequencies and also the first rate constants for the OH-oxidation of two carbonyl nitrates: 4-nitrooxy-2-butanone and 5-nitrooxy-2-pentanone.

2 Experimental section

2.1 Reactants syntheses

As a usual OH precursor in simulation chamber experiments, isopropyl nitrite was synthesized by dropwise addition of a dilute solution of H$_2$SO$_4$ into a mixture of NaNO$_2$ and isopropanol following the classical protocol proposed by Taylor et al. (1980).

On the contrary, 4-nitroxy-2-butanone and 5-nitroxy-2-pentanone were synthesized for the first time. A great

110 care was taken to the development of a robust process: 4-nitroxy-2-butanone and 5-nitroxy-2-pentanone syntheses are based on Kames' method (Kames et al., 1993). This method consists in a liquid/gas phase reaction

112 where the corresponding hydroxy-ketone reacts with NO_3 radicals released from the dissociation of N_2O_5. N_2O_5 was preliminarily synthesized in a vacuum line by reaction of NO_2 with ozone, as described by Scarfogliero et

114 al. (2006). The synthesis of the carbonyl nitrate is performed in a dedicated vacuum line connected to two bulbs, one containing the hydroxy-ketone, the other one containing N_2O_5. The two bulbs are also connected to each

116 other. In a first step, the bulbs are placed in a liquid N_2 cryogenic trap and pumped in order to remove air and impurities. In a second step, the cryogenic trap is removed from the bulb containing N_2O_5 in order to let it warm

118 and transfer into the bulb containing the hydroxy-ketone. Then, the bulb containing both reactants is stirred and kept at ice temperature for approximatively 1h. Finally, the resulting carbonyl nitrate and nitric acid, its co-

120 product, were separated by liquid-liquid extraction using dichloromethane and water. The carbonyl nitrate structure and purity were verified by FT-IR and GC-MS. Traces of impurities (HCOOH and CH_3COOH) have

122 been detected. The carbonyl nitrates were stored at -18° C and under nitrogen atmosphere to prevent them from decomposition. Infrared spectra of 4-nitroxy-2-butanone and 5-nitroxy-2-pentanone are available on

124 EUROCHAMP Data Centre (https://data.eurochamp.org).

2.2 Determination of photolysis frequencies

126 The photolysis frequencies of the two carbonyl nitrates were determined by carrying out experiments in the CESAM simulation chamber which is only briefly described here as detailed information can be found in Wang

128 et al. (2011). The chamber consists of a 4.2 m^3 stainless steel vessel equipped with a multiple reflection optical system interfaced to a FTIR spectrometer (Bruker Tensor 37) and also with NO, NO_2 and O_3 analyzers (Horiba)

130 to monitor the composition of the gas phase. The chamber is also equipped with three high pressure xenon arc lamps (MH-Diffusion, MacBeam 4000) which are combined with 7 mm Pyrex filters. This irradiation device

132 provides a very realistic actinic flux (see comparison with the solar actinic flux in Figure S1) which allows measuring photolysis frequencies under realistic conditions (Wang et al., 2011; Suarez-Bertoa et al., 2012).

134 However, since the intensity of the irradiation in CESAM chamber is lower than the one in ambient environment, $j_{nitrate}/j_{NO2}$ were provided in order to allow calculating $j_{nitrate}$ under various sunlight conditions.

136 Hence, the intensity of the actinic flux was determined by measuring the photolysis frequency of NO_2 (J_{NO2}) during dedicated experiments. 400 ppbv of NO_2 in 1000 mbar of N_2 were injected into CESAM chamber and

138 kept in the dark for 20 min. The lights were then turned on during 20 min, and finally the mixture was left in the dark for an additional 20 min period. The photolysis frequency was subsequently determined using a kinetic

140 numeric model developed for previous NOx photo-oxidation experiments in CESAM (Wang et al., 2011). The fitting of modeled values from the measured data provided a NO_2 photolysis frequency equal to 2.2×10^{-3} s^{-1} (±

142 0.01, 2σ error).

During a typical experiment, carbonyl nitrates were introduced into the chamber which was preliminarily filled

144 at atmospheric pressure with N_2/O_2 (80/20). For the injection, the bulb containing the carbonyl nitrate was connected to the chamber and slightly heated while it was flushed with N_2. Mixing ratios of carbonyl nitrates

146 ranged from hundreds ppb to ppm. Because carbonyl nitrates may decompose during the injection, large amounts of NO_2 (hundreds ppb) were present in the mixture. Cyclohexane was also added to the mixture as an OH-

148 scavenger with mixing ratios of approx. 4 ppm. Considering the fact that cyclohexane is approximatively twice more reactive with OH radicals than the carbonyl nitrates (see Results section), it was estimated that between 80

150 and 98% of the OH radicals were scavenged (depending on the experiment considered). The mixture was kept under dark conditions during two hours to be able to assess the impact of the reactor's walls and to minimize

152 their effects by passivation. Then, the mixture was irradiated during 3 hours. For most experiments, the mixture was finally left in the dark for approximately 1 hour after the irradiation period to allow for verifying if wall

154 losses were constant during the entire duration of the experiment.

During the experiment, the carbonyl nitrate loss processes can be described as:

156 Carbonyl nitrate (walls) $\rightarrow$ products   (k)   (2a)

Carbonyl nitrate + hν $\rightarrow$ products   ($j_{nitrate}$)   (2b)
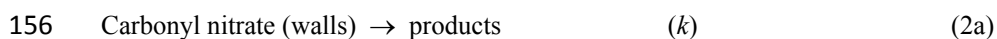
158 $-\dfrac{d[nitrate]}{dt} = (j_{nitrate} + k) \times [nitrate]$ (Eq. 1)

$ln[nitrate]_t = ln[nitrate]_0 - (k + j_{nitrate}) \times t$ (Eq. 2)

160 The reaction (2a) had to be added to the system to take into account the interaction or adsorption of the carbonyl nitrates on the stainless steel walls of CESAM during the experiments. By plotting ln[nitrate]$_t$ *vs*. time, where

162 [nitrate]$_t$ is the concentration of the carbonyl nitrate at time t, a straight line is obtained with a slope of (k + $j_{nitrate}$). The same approach was applied to each of the 'dark' periods, before and after irradiation, to determine

164 their respective dark decay rates, namely k_{before} and k_{after} and k was calculated as the average of k_{before} and k_{after} for each experiment. Finally, $j_{nitrate}$ was calculated as the difference between the loss rate during the irradiation

166 period (k + $j_{nitrate}$) and the averaged loss rate during the dark periods (k).

The uncertainties were calculated by adding the respective statistical errors (2σ) associated to the dark and light

168 periods, the former set as the average of the uncertainties determined for both dark periods (i.e., before and after irradiation). However, for some experiments, it was observed that the dark decay rate before irradiation was

170 significantly higher than the one after, suggesting that wall loss process is more complex than a "simple" first order process and may decrease with time due to a passivation of the walls. More generally, interactions of gases

172 with walls remain poorly understood and are currently subject to intensive investigations by the scientific community. Here, in order to determine wall loss decays which are as representative as possible of the one

174 during the irradiation period, the first experimental points (after the injection of the carbonyl nitrate) were not taken into account for the linear fit leading to the determination of k_{before}. In addition, the uncertainty was not

176 calculated using the approach detailed above, the statistical error being too low compared to the difference between k_{before} and k_{after}. The uncertainty was thus estimated in order to include the lowest and the highest $J_{nitrate}$

178 values calculated with the highest and the lowest k value, respectively. Finally, the overall uncertainty associated with the photolysis frequency of each of the carbonyl nitrates was calculated as the average of the uncertainties

180 obtained for each experiment, divided by the square root of the number of experiments (2 or 3).

2.3 Determination of the OH-oxidation rate constants

The kinetic experiments for the OH-oxidation of the carbonyl nitrates were performed in the CSA chamber at room temperature and atmospheric pressure, in a mixture of N_2/O_2 (80/20). The chamber consists of a 977 L Pyrex^{TM} vessel irradiated by two sets of 40 fluorescent tubes (Philips TL05 and TL03) that surround the chamber. The emissions of these black lamps are centered on 360 and 420 nm, respectively. The chamber is equipped with a multiple reflection optical system with a path length of 180 m interfaced to a FTIR spectrometer (Vertex 80 from Bruker). Additional details about this smog chamber are given elsewhere (Doussin et al., 1997; Duncianu et al., 2017).

The relative rate technique was used to determine the rate constant for the OH-oxidation of the carbonyl nitrates with methanol as reference compound. We used the IUPAC recommended value $k_{(methanol+OH)} = (9.0 \pm 1.8) \times 10^{-13}$ cm^3 molecule^{-1} s^{-1} (http://www.iupac-kinetic.ch.cam.ac.uk/). Hydroxyl radicals were generated by photolyzing isopropyl nitrite. Initial mixing ratios of reactants (carbonyl nitrate, isopropyl nitrite, methanol and NO) were in the ppm range. As previously described, the carbonyl nitrate was introduced into the chamber by connecting the bulb to the chamber and by slightly heating and flushing it with N_2. NO was added to the mixture in order to enhance the formation of OH radicals by reaction with HO_2 radicals which are formed by isopropyl nitrite photolysis. All experiments were conducted during a 1 h period of continuous irradiation.

Prior to the experiments, it was verified that photolysis and wall losses of the studied compounds were negligible under our experimental conditions. This can be explained by the facts that i) the irradiation system of CSA chamber emits photons at significantly higher wavelengths than the one of CESAM chamber, and ii) the walls of the chamber are made of Pyrex which is more chemically inert than stainless steel. It was therefore assumed that reaction with OH is the only fate of both, the studied compound (carbonyl nitrate) and the reference compound (methanol) and that neither of these compounds is reformed at any stage during the experiment. Based on these hypotheses, it can be shown that (Atkinson, 1986):

$$ln\frac{[nitrate]_0}{[nitrate]_t} = \frac{k_{nitrate}}{k_{methanol}} \times \frac{[methanol]_0}{[methanol]_t} \qquad\qquad (Eq. 3)$$

where [nitrate]$_0$ and [methanol]$_0$, and [nitrate]$_t$ and [methanol]$_t$ stand for the concentration of the carbonyl nitrate and the reference compound at times 0 and t, respectively. The plot ln([nitrate]$_0$/[nitrate]$_t$) *vs.* ln([methanol]$_0$/[methanol]$_t$) is linear with a slope equal to $k_{nitrate}/k_{methanol}$ and an intercept of zero. The uncertainty on $k_{nitrate}$ was calculated by adding the relative uncertainty corresponding to the statistical error on the linear regression (2σ) and the error on the reference rate constant (here 20 % for methanol).

2.4 Chemicals and gases

Dry synthetic air was generated using N_2 (from liquid nitrogen evaporation, >99.995% pure, <5 ppm H_2O, Linde Gas) and O_2 (quality N45, >99.995% pure, <5 ppm H_2O, Air Liquide). Chemicals obtained from commercial sources are: NO (quality N20, >99% Air Liquide), NO_2 (quality N20, >99% Air Liquide), 4-hydroxy-2-butanone (95% Aldich), 5-hydroxy-2-pentanone (95% Aldich), cyclohexane (VWR), methanol (J.T. Baker), H_2SO_4 (95% VWR), $NaNO_2$ ($\geq$99 Prolabo), isopropanol (VWR).

3 Results and discussion

3.1 Photolysis of carbonyl nitrates

218   Figure 1 presents the kinetic plots obtained for the two compounds, where ln[nitrate] was plotted as a function of time. A significant decrease was observed for both compounds during the dark period, before and after

220   irradiation, suggesting that they adsorb or decompose on the walls. Photolysis frequencies were thus calculated as the difference between the decay rates in the dark and the one under irradiation (see section 2.2). Results

222   obtained for both compounds and for all experiments are given in Table 1. For 4-nitrooxy-2-butanone, photolysis frequencies are in good agreement despite the fact that decay rates in the dark differ from an experiment to

224   another. For 5-nitrooxy-2-butanone, it can be seen that the decay rate in the dark before irradiation is significantly higher than the one after (in particular for experiments 3 and 4), suggesting that wall losses may

226   decrease with time due to a passivation of the walls. Despite this, comparison of the three experiments showed good agreement. For CESAM irradiation conditions, the photolysis frequencies are $(1.3 \pm 0.2) \times 10^{-5}$ s^{-1} for 4-

228   nitrooxy-2-butanone and $(0.7 \pm 0.2) \times 10^{-5}$ s^{-1} for 5-nitrooxy-2-pentanone. Hence, $j_{nitrate}/j_{NO2}$ were found to be $(5.9 \pm 0.9) \times 10^{-3}$ for 4-nitrooxy-2-butanone and $(3.2 \pm 0.9) \times 10^{-3}$ for 5-nitrooxy-2-pentanone.

230   These photolysis frequencies have been compared in Table 2 to those we obtained in a previous study (Suarez-Bertoa et al., 2012) for 3-nitrooxy-2-propanone, 3-nitrooxy-2-butanone and 3-methyl-3-nitrooxy-2-butanone

232   using the same experimental conditions and methodology. Experimental photolysis frequencies have also been compared to those calculated using cross sections published in the literature and by assuming a quantum yield

234   equal to unity. The intensity of the actinic flux in CESAM chamber was determined by combining measurement of the spectrum of the lamps with a spectroradiometer and determination of j_{NO2} by chemical actinometry (see

236   section 2.2). For 3-nitrooxy-2-propanone and 3-nitrooxy-2-butanone, cross sections were taken from Barnes et al. (1993). For 4-nitrooxy-2-butanone and 5-nitrooxy-2-pentanone, for which no data have been provided in the

238   literature, cross sections were estimated using those for corresponding monofunctional species and by applying the enhancement factor (r_{nk}) obtained for 3-nitrooxy-2-propanone (Müller et al., 2014):

240     $$r_{nk} = \frac{s_{nk}}{s_n + s_k} \qquad\qquad\qquad\qquad\qquad \text{(Eq.4)}$$

    Where s_{nk}, s_n and s_k are the absorption cross sections of the keto nitrate, the alkyl nitrate and the ketone,

242   respectively. For 4-nitrooxy-2-butanone, cross sections of 2-butanone and 1-butyl nitrate were taken from IUPAC, 2006. For 5-nitroxy-2-pentanone, cross sections of 2-pentanone (http://satellite.mpic.de/spectral_atlas)

244   and 1-pentyl nitrate (Clemitshaw et al., 1997) were used. From these results, it can be observed that the experimental photolysis frequencies (j_{exp}) obtained for 3-nitrooxy-2-propanone and 4-nitrooxy-2-butanone are

246   very close and can be considered as equal within uncertainties. This suggests that the strong enhancement in the cross sections induced by the interaction between the two functional groups, which has been observed for α-

248   nitrooxy ketones, also exists with the same amplitude for β-nitrooxy ketones. This is confirmed by the fact the experimental value for 4-nitrooxy-2-butanone is in very good agreement with the calculated value, obtained by

250   assuming that the enhancement factor is the same as the one for 3-nitrooxy-2-propanone. This effect, nonetheless, seems to fade away when the two functions are one carbon further away: The experimental

252   photolysis frequency obtained for 5-nitrooxy-2-pentanone is indeed significantly lower than those for 3-nitrooxy-2-propanone and 4-nitrooxy-2-butanone. It is also much lower than the J value calculated by assuming

254   the same enhancement factor as for 3-nitrooxy-2-propanone. This result suggests that the enhancement is

significantly reduced for γ-nitrooxy ketones even if it is probably not totally absent. This can easily be explained by the fact that the inductive effect of the nitrate group is expected to decrease when the distance between the functional groups increases. Another explanation would be that the quantum yield is significantly lower than unity. Finally, by comparing results for 3-nitrooxy-2-propanone, 3-nitrooxy-2-butanone and 3-methyl-3-nitrooxy-2-butanone, it can be observed that photolysis frequencies increase with the substitution of the alkyl chain. From these kinetic data, it can be concluded that photolysis frequencies of α- and β-nitrooxy ketones are much higher than those obtained when considering the sum of the photolysis frequencies for monofunctional species.

Products formed by the photolysis of the carbonyl nitrates were investigated by FTIR spectrometry. For both compounds, only peroxy acetyl nitrate (PAN) was detected. To calculate its formation yield, concentration of PAN was plotted as a function of $-\Delta[\text{nitrate}]_{\text{photolysis}}$, i.e., the carbonyl nitrate loss rate due to photolysis. This one was calculated by subtracting the loss rate measured during the dark period before the photolysis to the one measured during the photolysis. Because the yield was calculated as the initial slope of the plot, it was considered that the dark period before irradiation was more representative than the one after. The uncertainty on the yield was calculated by taking into account the uncertainties on the infrared absorption cross sections of PAN (10%) and carbonyl nitrates (10%) as well as the uncertainty on j (see table 1). For 5-nitrooxy-2-pentanone, this uncertainty is quite large because the photolysis rate is relatively slow in comparison to loss to the reactor walls. PAN formation yields obtained for both compounds are given in Table 1.

For 4-nitrooxy-2-butanone, PAN is formed with a yield equal to unity. Its formation can be explained by the dissociation of the C(O)-C bond as shown in Scheme 1. This pathway also leads to the formation of the alkyl radical $^{\bullet}\text{CH}_2\text{-CH}_2\text{ONO}_2$ which reacts with O_2 to form the corresponding peroxy radical, this latter evolving to the formation of the alkoxy by reaction with NO. Two pathways have been considered for the evolution of the alkoxy radical: i) the decomposition which may lead to the formation of NO_2 and two molecules of HCHO and ii) the reaction with O_2 which produces nitrooxy ethanal, also called ethanal nitrate ($CH_2(ONO_2)\text{-CH(O)}$). None of these two products have been detected by FTIR. However, absorption bands of ethanal nitrate are expected to be very similar to those of the reactant and it may thus be difficult to distinguish them. In addition, ethanal nitrate is expected to photodissociate much faster than the keto nitrate. The other photodissociation pathway is the cleavage of the $O\text{-}NO_2$ bond. It leads to the formation of the radical $CH_3C(O)CH_2CH_2O^{\bullet}$ which is expected to react with O_2 to form a dicarbonyl product. This product was not observed and this is in good agreement with the formation of PAN with a yield equal to unity by the other photodissociation pathway. It should be noticed that PAN has been detected as a primary product suggesting that its formation via the photolysis of the dicarbonyl product is not expected. In our experiments, it was not possible to measure NO_2 formation yield because large amounts of NO_2 (hundreds ppb) were introduced with the carbonyl nitrate (probably due to its decomposition during the injection).

As discussed above, since the enhancement in the cross sections is larger at the higher wavelengths, where absorption by the nitrate chromophore is very small, it was proposed by Müller et al. (2014) that the absorption by the carbonyl chromophore is enhanced due to the neighboring nitrate group. The authors also suggest that the photodissociation proceeds by a dissociation of the weak $O\text{-}NO_2$ bond, i.e. that a photon absorption by one chromophore (carbonyl group) causes dissociation in another part of the molecule (nitro group). This is not in

294 line with what we observed in our study. From our experiments, we conclude that the photolysis of 4-nitrooxy-2-butanone proceeds mainly by a dissociation of the C(O)-C bond. In the former study on the photolysis of 3-
296 nitrooxy-2-propanone, 3-nitrooxy-2-butanone and 3-methyl-3-nitrooxy-2-butanone (Suarez-Bertoa et al., 2012), PAN and carbonyl compounds (respectively, formaldehyde, acetaldehyde and acetone) were detected as major
298 products. However, branching ratio of the two pathways (dissociation of O-NO_2 and C(O)-C bonds) could not be determined as the formation of these products, in particular PAN, can be explained by the two pathways.

300 For 5-nitrooxy-2-pentanone, formation yield of PAN has been observed to be much lower: 0.16 ± 0.08. As for 4-nitrooxy-2-butanone, its formation can be explained by the dissociation of the C(O)-C bond (see Scheme 2). This
302 result suggests that both dissociation pathways may occur and that O-NO_2 dissociation could be the major one. However, this was not confirmed by the detection of the dicarbonyl compound (2-oxo-pentanal) which is
304 expected to be formed by this pathway. Despite the fact that no standard was available for this compound, no characteristic band was observed in the residual spectrum (after subtraction of reactants and PAN spectra).
306 Because the photolysis rate of 5-nitrooxy-2-pentanone is very low, we suspect that the concentration of this product is below the detection limit. Nevertheless, the low PAN yield is a strong indication that O-NO_2
308 dissociation may be the major pathway, contrary to what has been observed for 4-nitrooxy-2-butanone. This should be considered in the light of the low enhancement of absorption cross sections which has been assumed
310 for this compound. Hence, in the case of γ-nitrooxy ketones, the enhancement of the absorption by the carbonyl chromophore seems to significantly decrease, leading to a lower branching ratio of the C(O)-C bond
312 dissociation.

3.2 OH-oxidation of carbonyl nitrates

314 Rate constants of the OH-oxidation have been measured for 4-nitrooxy-2-butanone and 5-nitrooxy-2-pentanone. Prior to the experiments, it was checked that the carbonyl nitrates do not photolyse nor decompose/adsorb on the
316 walls of the chamber. Figure 2 represents the kinetic plots obtained for the two carbonyl nitrates. For each compound, several independent kinetic experiments were performed and data were combined to provide the
318 $k_{ketonitrate}/k_{methanol}$ for each compound (see Figure 3). In order to limit errors in the quantification of reactants due to the possible formation of carbonyl nitrates as products, only the very beginning of the experiments was taken
320 into account for the kinetic plots. This explains the small number of experimental points. The obtained rate constants are given in Table 3. These data are, to our knowledge, the first determinations of the rate constants for
322 the reaction of OH with these two carbonyl nitrates. From these data, it can be concluded that 4-nitrooxy-2-butanone and 5-nitrooxy-5-pentanone have similar reactivity towards OH radicals with rate constants equal to
324 $(2.9 \pm 1.0) \times 10^{-12}$ and $(3.3 \pm 0.9) \times 10^{-12}$ cm^3 molecule^{-1} s^{-1}, respectively.

325 Rate constants provided in this study, as well as those previously reported for a series of α-nitrooxy-ketones
326 (Suarez-Bertoa et al., 2012) have been compared to those estimated using structure-activity relationships (SARs) in Table 4. Different SARs have been evaluated: i) the one developed by Kwok and Atkinson (1995) with
328 updated factors F(-ONO_2) = 0.14 and F(-C-ONO_2) = 0.28 from Bedjanian et al. (2018); ii) the one developed by Kwok and Atkinson (1995) with updated factors F(-ONO_2) = 0.8 and F(-C-ONO_2) = 0.1 from Suarez-Bertoa et
330 al. (2012); iii) the one developed by Neeb (2000) which proposes a different type of parametrization and has been observed to be particularly accurate for oxygenated species; and iv) the one developed by Jenkin et al.

332 (2018) which proposes a parametrization very similar to the one from Kwok and Atkinson (1995) and Bedjanian et al. (2018). The rate constant for 5-nitrooxy-2-pentanone is reasonably well reproduced by all SARs (within a

334 factor of 2). For 4-nitrooxy-2-butanone, only the parametrization provided by Suarez-Bertoa et al. (2012) succeeds in reproducing the experimental value. This can be explained by the fact that this parametrization has

336 been optimized for carbonyl nitrates while the others have been developed using the entire dataset for compounds containing a nitrate group ($-ONO_2$) (Jenkin et al., 2018) or using the dataset for alkyl nitrates

338 (Bedjanian et al., 2018). The main difference between these parametrizations is that in Suarez-Bertoa et al. (2012), the factor $F(-ONO_2)$ is much less deactivating than for the others. This could result from electronic

340 interactions between the two functional groups. However, Suarez-Bertoa et al. (2012) noticed that their parametrization gives poor results for alkyl nitrates, suggesting that a specific parametrization has to be used for

342 multifunctional species. This also suggests that the principle of SARs based on the group additivity method may not be suitable for multifunctional molecules.

344 From these experiments, several oxidation products have been detected: HCHO, PAN and methylglyoxal for 4-nitrooxy-2-butanone, and HCHO, PAN and 3-nitrooxy-propanal for 5-nitrooxy-2-pentanone. However, their

346 quantification was highly uncertain because the infrared spectra were complex due to the presence of methanol, isopropyl nitrite, impurities (in particular acetic acid) and their oxidation products. Dedicated mechanistic

348 experiments should now/in the near future be performed using HONO as OH source in order to simplify the chemical mixture.

350 **3.3 Atmospheric implications**

Atmospheric lifetimes of the investigated compounds are presented in Table 5. The photolysis frequencies were

352 estimated using $j_{nitrate}/j_{NO2}$ ratios measured in this study and using j_{NO2} for typical tropospheric irradiation conditions corresponding to the 1st July at noon and at 40° latitude North (overhead ozone column: 300, albedo:

354 0.1; aerosol optical depth: 0.235; cloud optical depth: 0 ; TUV NCAR Model, http://www.cprm.acd.ucar.edu/Models/TUV/Interactive_TUV/). For $j_{NO2} = 1.03 \times 10^{-2}$ s^{-1}, photolysis frequencies

356 of carbonyl nitrates are: $(6.1 \pm 0.9) \times 10^{-5}$ s^{-1} for 4-nitrooxy-2-butanone and $(3.3 \pm 0.9) \times 10^{-5}$ s^{-1} for 5-nitrooxy-2-pentanone. Under these irradiation conditions, lifetimes ($\tau_{hv} = 1/j$) were found to be 4 and 8 hours,

358 respectively. For OH-oxidation, lifetimes ($\tau_{OH} = (1/(k_{OH}[OH]))$) were calculated using typical OH concentrations of 2×10^6 molecule cm^{-3} (Atkinson and Arey, 2003). They are both equal to approximatively two days. Hence, it

360 appears that for 4-nitrooxy-2-butanone and for 5-nitrooxy-2-pentanone, photolysis is a more efficient sink than oxidation by OH radicals. An identical conclusion was obtained for α-nitrooxy carbonyls (Suarez-Bertoa et al.,

362 2012; Barnes et al., 1993; Zhu et al., 1991). However, OH-initiated oxidation is not negligible, especially under polluted conditions where OH concentrations can be higher than 1×10^7 molecule cm^{-3}.

364 In order to evaluate the impact of these carbonyl nitrates on the nitrogen budget and the transport of NOx, it is crucial to determine whether their atmospheric sinks, here mainly photolysis, release NO_2 or not. For 4-nitrooxy-

366 2-butanone, we observed that the photolysis proceeds mainly by a dissociation of the C(O)-C bond which does not necessarily lead to the release of NO_2 (see Scheme 2). In our experimental conditions (i.e., with high NO_2

368 mixing ratios), this pathway leads to the formation of PAN which was detected with a yield equal to unity. Under more realistic NO/NO_2 ratio, this reaction may also produce HCHO and CO_2. The co-products of PAN,

370   which could not be detected in our study, are expected to be formaldehyde + NO_2 or ethanal nitrate. One NO_2 molecule is hence released in the first hypothesis. Ethanal nitrate may react and undergo photolysis even faster

372   than nitrooxy ketones and may thus lead to NO_2 release quite rapidly. However, as data on the reactivity of ethanal nitrate are not available in the literature, one cannot provide a definite conclusion. In the case of 5-

374   nitrooxy-2-pentanone, the dissociation of the C(O)-C bond has been observed to be a minor pathway suggesting that the major one, which was not directly observed here, is the O-NO_2 dissociation. This process certainly leads

376   to the release of NO_2.

4 Conclusions

378   This paper presents the first study on the atmospheric reactivity of 4-nitrooxy-2-butanone and 5-nitrooxy-2-pentanone. Thanks to experiments in simulation chambers, photolysis frequencies and rate constants of the OH-

380   oxidation were measured for the first time. From these results, it is concluded that, similarly to α-nitrooxy ketones, β-nitrooxy ketones have enhanced UV absorption cross sections and quantum yields equal or close to

382   unity, making photolysis a very efficient sink for these compounds. Results obtained for 5-nitrooxy-2-pentanone which is a γ-nitrooxy ketone, suggest a lower enhancement of cross sections leading to slightly longer

384   atmospheric lifetimes. This can easily be explained by the increasing distance between the two chromophore groups. Some photolysis products were also detected allowing estimating the branching ratio between the two

386   possible pathways, i.e., the dissociation of the C(O)-C bond and the one of the O-NO_2 bond. For 4-nitrooxy-2-butanone, we conclude that the photolysis proceeds mainly by a dissociation of the C(O)-C bond which does not

388   necessarily lead to the release of NO_2. In the case of 5-nitrooxy-2-pentanone, our results suggest that the dissociation of the O-NO_2 bond is the major pathway. Reactivity of 4-nitrooxy-2-butanone and 5-nitrooxy-2-

390   pentanone with OH radicals was also investigated. Both compounds have similar reactivity towards OH radicals leading to lifetimes of approximatively two days. Experimental rate constants are in good agreement with those

392   estimated by the SAR proposed by Kwok and Atkinson (1995) when using the parametrization proposed by Suarez-Bertoa et al. (2012) for carbonyl nitrates. However, this specific parametrization does not allow

394   reproducing experimental data for monofunctional alkyl nitrates, suggesting that specific parametrization should be used for multifunctional species. Finally, these compounds are expected to be removed from the atmosphere

396   fairly rapidly and to act as (only) temporary reservoirs of NOx. If formed during the night, they could however contribute to longer range transport of NOx.

398   *Author contributions*

BPV coordinated the research project. BPV, RSB and JFD designed the experiments in simulation chambers.

400   RSB performed the experiments with the technical support of MC and EP. RSB and MDa performed the organic syntheses. BPV, RSB and MDu performed the data treatment and interpretation. BPV and RSB wrote the paper

402   and BPV was in charge of its final version. All coauthors revised the manuscript content, giving final approval of the version to be submitted.

404   *Competing interests*

The authors declare that they have no conflict of interest.

406   *Acknowledgments*

This work was supported by the French National Agency for Research (Project ONCEM-ANR-12-BS06-0017-
408   01) and by the European Union within the 7th Framework Program, section "Support for Research
Infrastructure-Integrated Infrastructure Initiative" through EUROCHAMP-2 project (RII3-CT-2009-228335) and
410   the Horizon 2020 Research and Innovation Program through the EUROCHAMP-2020 Infrastructure Activity
under grant agreement no. 730997. The authors thank Mila Ródenas (mila@ceam.es) (CEAM, Paterna-Valencia,
412   Spain) for the development and the free distribution of the software ANIR through the EUROCHAMP-2020
Data Centre website (https://data.eurochamp.org).

414   **References**

Atkinson, R., and Arey, J.: Gas-phase tropospheric chemistry of biogenic volatile organic compounds: a
416   review, Atmos. Environ., 37, 197-219, 2003.

Barnes, I., Becker, K. H., and Zhu, T.: Near UV absorption spectra and photolysis products of
418   difunctional organic nitrates: possible importance as NOx Reservoirs, J. Atmos. Chem., 17, 353-373,
1993.

420   Bean, J. K., and Hildebrand Ruiz, L.: Hydrolysis and gas-particle partitioning of organic nitrates formed
from the oxidation of α-pinene in environmental chamber experiments, Atmos. Chem. Phys. 15, 20629-
422   20653, 2015.

Beaver, M. R., St Clair, J. M., Paulot, F., Spencer, K. M., Crounse, J. D., LaFranchi, B. W., Min, K. E.,
424   Pusede, S. E., Wooldridge, P. J., Schade, G. W., Park, C., Cohen, R. C., and Wennberg, P. O.:
Importance of biogenic precursors to the budget of organic nitrates: observations of multifunctional
426   organic nitrates by CIMS and TD-LIF during BEARPEX 2009, Atmos. Chem. Phys., 12, 5773-5785,
2012.

428   Bedjanian, Y., Morin, J., and Romanias, M. N.: Reactions of OH radicals with 2-methyl-1-butyl,
neopentyl and 1-hexyl nitrates. Structure-activity relationship for gas-phase reactions of OH with alkyl
430   nitrates: An update, Atmos. Environ., 180, 167-172, 2018.

Clemitshaw, K. C., Williams, J., Rattigan, O. V., Shallcross, D. E., Law, K. S., and Cox, R. A.: Gas-
432   phase ultraviolet absorption cross-sections and atmospheric lifetimes of several C2-C5 alkyl nitrates, J.
Photochem. Photobiol. A, 102, 117-126, 1997.

434   Doussin, J. F., Ritz, D., Durand-Jolibois, R., Monod, A., and Carlier, P.: Design of an environmental
chamber for the study of atmospheric chemistry: New developments in the analytical device, Analusis,
436   25, 236-242, 1997.

Duncianu, M., David, M., Kartigueyane, S., Cirtog, M., Doussin, J. F., and Picquet-Varrault, B.:
438   Measurement of alkyl and multifunctional organic nitrates by Proton Transfer Reaction Mass
Spectrometry, Atmos. Meas. Tech., 10, 1445-1463, 2017.

440   Finlayson-Pitts, B. J., and Pitts Jr., J. N.: Chemistry of the Upper and Lower Atmosphere, Academic
Press, San Diego, 2000.

442   Horowitz, L. W., Fiore, A. M., Milly, G. P., Cohen, R. C., Perring, A., Wooldridge, P. J., Hess, P. G., Emmons, L. K., and Lamarque, J.-F.: Observational constraints on the chemistry of isoprene nitrates over
444   the eastern United States, J. Geophys. Res., 112, D12S08, 2007.

Ito, A., Sillman, S., and Penner, J. E.: Effects of additional nonmethane volatile organic compounds,
446   organic nitrates, and direct emissions of oxygenated organic species on global tropospheric chemistry, Journal of Geophysical Research-Atmospheres, 112, 10.1029/2005jd006556, 2007.

448   Jenkin, M. E., Valorso, R., Aumont, B., Rickard, A. R., and Wallington, T. J.: Estimation of rate coefficients and branching ratios for gas-phase reactions of OH with aliphatic organic compounds for use
450   in automated mechanism construction, Atmos. Chem. Phys., 18, 9297-9328, 10.5194/acp-18-9297-2018, 2018.

452   Kames, J., Schurath, U., Flocke, F., and Volz-Thomas, A.: Preparation of organic nitrates from alcohols and N_2O_5 for species identification in atmospheric samples, J. Atmos. Chem., 16, 349-359, 1993.

454   Kwok, E. S. C., and Atkinson, R.: Estimation of Hydroxyl Radical Reaction Rate Constants for Gas-Phase Organic Compounds using a Structure-Reactivity Relationship: an update, Atmos. Environ., 29,
456   1685-1695, 1995.

Mao, J. Q., Paulot, F., Jacob, D. J., Cohen, R. C., Crounse, J. D., Wennberg, P. O., Keller, C. A.,
458   Hudman, R. C., Barkley, M. P., and Horowitz, L. W.: Ozone and organic nitrates over the eastern United States: Sensitivity to isoprene chemistry, Journal of Geophysical Research-Atmospheres, 118, 11256-
460   11268, 10.1002/jgrd.50817, 2013.

Muller, J. F., Peeters, J., and Stavrakou, T.: Fast photolysis of carbonyl nitrates from isoprene, Atmos.
462   Chem. Phys., 14, 2497-2508, 10.5194/acp-14-2497-2014, 2014.

Neeb, P.: Structure-Reactivity Based Estimation of the Rate Constants for Hydroxyl Radical Reactions
464   with Hydrocarbons, J. Atmos. Chem., 35, 295-315, 2000.

Ng, N. L., Brown, S. S., Archibald, A. T., Atlas, E., Cohen, R. C., Crowley, J. N., Day, D. A., Donahue,
466   N. M., Fry, J. L., Fuchs, H., Griffin, R. J., Guzman, M. I., Herrmann, H., Hodzic, A., Iinuma, Y., Jimenez, J. L., Kiendler-Scharr, A., Lee, B. H., Luecken, D. J., Mao, J. Q., McLaren, R., Mutzel, A.,
468   Osthoff, H. D., Ouyang, B., Picquet-Varrault, B., Platt, U., Pye, H. O. T., Rudich, Y., Schwantes, R. H., Shiraiwa, M., Stutz, J., Thornton, J. A., Tilgner, A., Williams, B. J., and Zaveri, R. A.: Nitrate radicals
470   and biogenic volatile organic compounds: oxidation, mechanisms, and organic aerosol, Atmos. Chem. Phys., 17, 2103-2162, 10.5194/acp-17-2103-2017, 2017.

472   Paulot, F., Crounse, J. D., Kjaergaard, H. G., Kroll, J. H., Seinfeld, J. H., and Wennberg, P. O.: Isoprene photooxidation: new insights into the production of acids and organic nitrates, Atmos. Chem. Phys., 9,
474   1479-1501, 10.5194/acp-9-1479-2009, 2009.

Perring, A. E., Bertram, T. H., Farmer, D. K., Wooldridge, P. J., Dibb, J., Blake, N. J., Blake, D. R.,
476   Singh, H. B., Fuelberg, H., Diskin, G., Sachse, G., and Cohen, R. C.: The production and persistence of Sigma $RONO_2$ in the Mexico City plume, Atmos. Chem. Phys., 10, 7215-7229, 10.5194/acp-10-7215-
478   2010, 2010.

Perring, A. E., Pusede, S. E., and Cohen, R. C.: An Observational Perspective on the Atmospheric
480   Impacts of Alkyl and Multifunctional Nitrates on Ozone and Secondary Organic Aerosol, Chemical Reviews, 113, 5848-5870, 10.1021/cr300520x, 2013.

482   Rindelaub, J. D., McAvey, K. M., and Shepson, P. B.: The photochemical production of organic nitrates from alpha-pinene and loss via acid-dependent particle phase hydrolysis, Atmos. Environ., 100, 193-201,

484   10.1016/j.atmosenv.2014.10.010, 2015.

Roberts, J. M.: The Atmospheric Chemistry of organic Nitrates, Atmos. Environ., 24A, 243-287, 1990.

486   Scarfogliero, M., Picquet-Varrault, B., Salce, J., Durand-Jolibois, R., and Doussin, J.-F.: Kinetic and Mechanistic Study of the Gas-Phase Reactions of a Series of Vinyl Ethers with the Nitrate Radical, J.

488   Phys. Chem. A, 110, 11074-11081, 2006.

Squire, O. J., Archibald, A. T., Griffiths, P. T., Jenkin, M. E., Smith, D., and Pyle, J. A.: Influence of

490   isoprene chemical mechanism on modelled changes in tropospheric ozone due to climate and land use over the 21st century, Atmos. Chem. Phys., 15, 5123-5143, 10.5194/acp-15-5123-2015, 2015.

492   Suarez-Bertoa, R., Picquet-Varrault, B., Tamas, W., Pangui, E., and Doussin, J. F.: Atmospheric Fate of a Series of Carbonyl Nitrates: Photolysis Frequencies and OH-Oxidation Rate Constants, Environ. Sci.

494   Technol., 46, 12502-12509, 10.1021/es302613x, 2012.

Taylor, W. D., Allston, T. D., Moscato, M. J., Fazenkas, G. B., Koslowski, R., and Takacs, G. A.:

496   Atmospheric Photodissociation lifetimes for nitromethane, methyl nitrite, and methyl nitrate., Int. J. Chem. Kinet., 12, 231-240, 1980.

498   Turberg, M. P., Giolando, D. M., Tilt, C., Soper, T., Mason, S., Davies, M., Klingensmith, P., and Takacs, G. A.: Atmospheric Photochemistry of Alkyl Nitrates, J. Photochem. Photobiol. A-Chem., 51,

500   281-292, 1990.

Wang, J., Doussin, J. F., Perrier, S., Perraudin, E., Katrib, Y., Pangui, E., and Picquet-Varrault, B.:

502   Design of a new multi-phase experimental simulation chamber for atmospheric photosmog, aerosol and cloud chemistry research, Atmospheric Measurement Techniques, 4, 2465-2494, 10.5194/amt-4-2465-

504   2011, 2011.

Xiong, F. L. Z., Borca, C. H., Slipchenko, L. V., and Shepson, P. B.: Photochemical degradation of

506   isoprene-derived 4,1-nitrooxy enal, Atmos. Chem. Phys., 16, 5595-5610, 10.5194/acp-16-5595-2016, 2016.

508   Zhu, T., Barnes, I., and Becker, K. H.: Relative-rate study of the gas-phase reaction of hydroxy radicals with difunctional organic nitrates at 298K and atmospheric pressure, J. Atmos. Chem., 13, 301-311,

510   1991.

512

514

Figure, scheme and table captions

516   **Scheme 1.** Photolysis pathways of 4-nitrooxy-2-butanone. Detected products are indicated with a grey background and their formation yield in given (in %).

518   **Scheme 2.** Photolysis pathways of 5-nitrooxy-2-pentanone. Detected products are indicated with a grey background and their formation yield in given (in %).

520   **Figure 1**. Kinetic plots for *(a)* the photolysis of 4-nitrooxy-2-butanone (experiment 2) and *(b)* the photolysis of 5-nitrooxy-2-pentanone (experiment 5). Red lines correspond to linear regressions.

522   **Figure 2.** Kinetic plots for the oxidation by OH radicals of 4-nitrooxy-2-butanone and 5-nitrooxy-2-pentanone. For 5-nitrooxy-2-pentanone, data have been shifted by 0.2 in y axis. Different symbols correspond to different

524   experiments.

    Table 1. Photolysis frequencies and PAN yields for 4-nitrooxy-2-butanone and 5-nitrooxy-2-pentanone

526   measured in CESAM chamber.

    Table 2. Comparison of experimental photolysis frequencies of carbonyl nitrates with those calculated for

528   CESAM irradiation conditions and by assuming a quantum yield equal to unity.

    Table 3. Rate constants for the OH-oxidation of 4-nitrooxy-2-butanone and 5-nitrooxy-2-pentanone.

530   **Table 4.** Comparison of experimental rate constants for the OH-oxidation of carbonyl nitrates with those estimated by SARs.

532   **Table 5.** Atmospheric lifetimes of carbonyl nitrates towards photolysis and reaction with OH radicals.

534
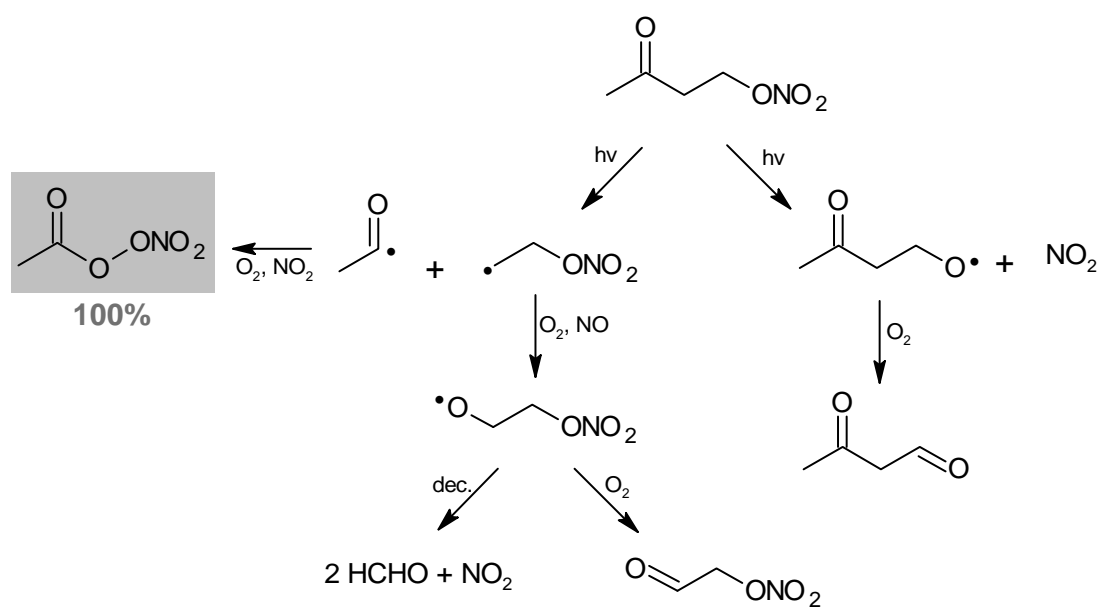
536

Scheme 1.

538
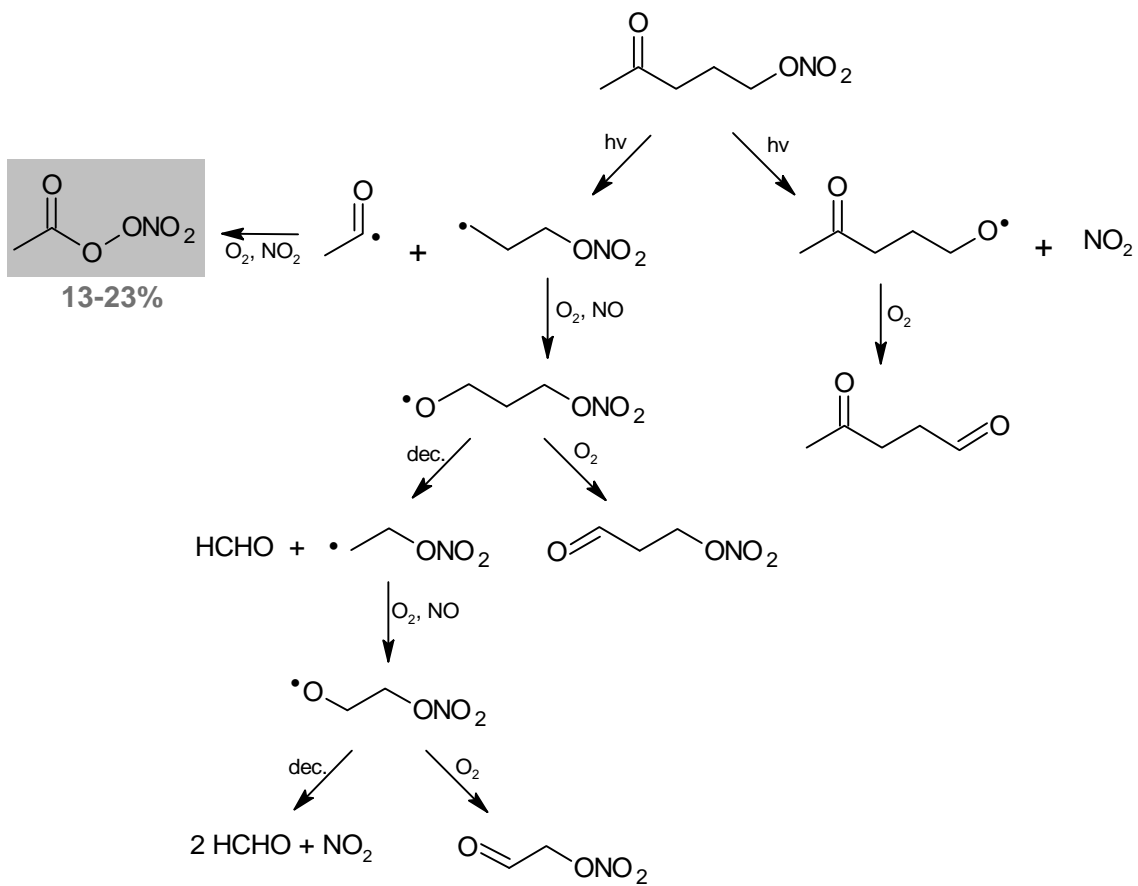
540   **Scheme 2.**

542

544

546

548
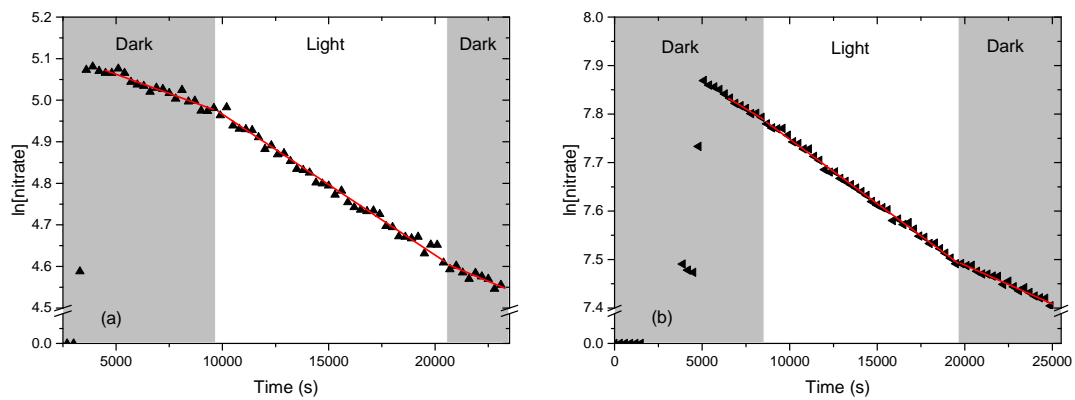
Figure 1.

550
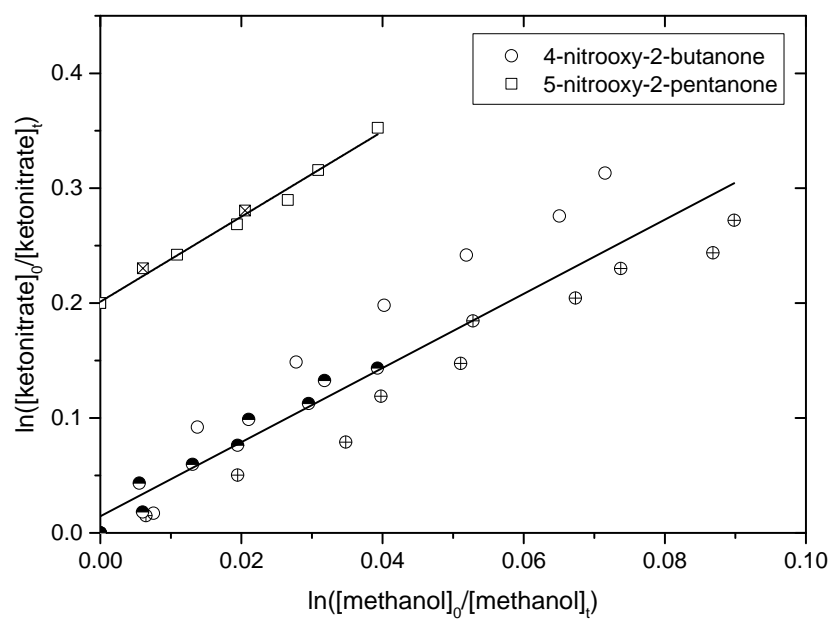
552   **Figure 2.**

Table 1.
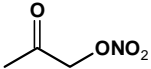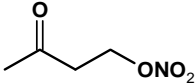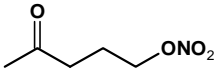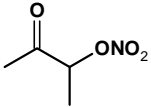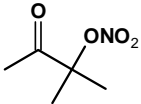
Compound	Experim.	k_{before} [a] $(\times 10^{-5}\ s^{-1})$	k_{after} [b] $(\times 10^{-5}\ s^{-1})$	$(k+j_{nitrate})$ [c] $(\times 10^{-5}\ s^{-1})$	$j_{nitrate}$ [d] $(\times 10^{-5}\ s^{-1})$	PAN yield (%)
4-nitrooxy-2-butanone	1	0.8 ± 0.1	-	2.1 ± 0.1	1.3 ± 0.2	100 ± 35
	2	1.9 ± 0.2	2.1 ± 0.1	3.3 ± 0.1	1.3 ± 0.3	100 ± 40
	Average				$\mathbf{1.3 \pm 0.2}$	$\mathbf{100 \pm 30}$
5-nitrooxy-2-pentanone	3	2.0 ± 0.2	1.1 ± 0.2	2.3 ± 0.1	0.7 ± 0.4	13 ± 9
	4	1.9 ± 0.2	1.1 ± 0.1	2.2 ± 0.1	0.7 ± 0.4	13 ± 9
	5	2.1 ± 0.2	1.6 ± 0.2	2.7 ± 0.1	0.8 ± 0.3	23 ± 13
	Average				$\mathbf{0.7 \pm 0.2}$	$\mathbf{16 \pm 8}$

554 [a, b] dark decay rate due to wall loss, before and after irradiation; [c] decay rate during irradiation period; [d] photolysis rate calculated as the difference between the decay rate during irradiation and

556 the average dark decay rate.

558

560

562 **Table 2.**

Compound	j_{exp} ($\times 10^{-5}$ s^{-1})	j_{calc} ($\times 10^{-5}$ s^{-1}) ($\phi=1$)
3-nitrooxy-2-propanone	1.5 ± 0.1 (Suarez-Bertoa et al., 2012)	1.4[b]
4-nitrooxy-2-butanone	1.3 ± 0.2 (This work)	1.6[a]
5-nitrooxy-2-pentanone	0.7 ± 0.2 (This work)	1.8[a]
3-nitrooxy-2-butanone	1.8 ± 0.1 (Suarez-Bertoa et al., 2012)	2.2[b]
3-methyl-3-nitrooxy-2-butanone	2.31 ± 0.05 (Suarez-Bertoa et al., 2012)	ND

[a] calculated with estimated cross sections (see text); [b] calculated with experimental cross sections

564 from literature;

Table 3.

Compound	$k_{nitrate}/k_{methanol}$	$k_{nitrate} \times 10^{-12}$ (cm^3 molecule^{-1} s^{-1})
4-nitrooxy-2-butanone	3.25 ± 0.47	2.9 ± 1.0
5-nitrooxy-2-pentanone	3.70 ± 0.28	3.3 ± 0.9

566 **Table 4.**

Compound	k_{exp} × 10⁻¹³	k_{SAR} Atkinson/Bedjanian[a] × 10⁻¹³	k_{SAR} Atkinson/Suarez[b] × 10⁻¹³	$k_{SAR Neeb}$[c] × 10⁻¹³	$k_{SAR Jenkin}$[d] × 10⁻¹³
3-nitrooxy-2-propanone	6.7[5]	2.0	6.6	5.8	2.5
3-nitrooxy-2-butanone	10.1[e]	4.5	13.2	6.8	3.7
3-methyl-3nitrooxy-2-butanone	2.6[e]	4.0	2.1	2.4	4.3
4-nitrooxy-2-butanone	29[f]	8.1	30.9	8.7	8.1
5-nitrooxy-2-pentanone	33[f]	21.4	22.5	47.6	19.5

568 Rate constants are expressed in cm^3 molecule⁻¹ s⁻¹; [a] SAR developed by Kwok and Atkinson (1995) with F(-ONO₂) and F(-C-ONO₂) from Bedjanian et al., 2018; [b] SAR developed by Kwok and Atkinson (1995) with F(-ONO₂) and F(-C-ONO₂) from Suarez-Bertoa et al., (2012) ;[c] SAR developed by Neeb (2000); [d] SAR developed 570 by Jenkin et al. (2018) ; [e] experimental data from Suarez-Bertoa et al. (2012); [f] This work.

Table 5.

Compound	$J \times 10^{-5\,a}$ (s^{-1})	$\tau_{h\nu}$ (hours)	$k_{OH} \times 10^{-12}$ (cm^3 molecule^{-1} s^{-1})	$\tau_{OH}{}^{b}$ (hours)
4-nitrooxy-2-butanone	6.1 ± 0.9	4	2.9 ± 1.0	48
5-nitrooxy-2-pentanone	3.3 ± 0.9	8	3.3 ± 0.9	42

572   [a] photolysis frequencies estimated for a typical solar actinic flux (40°N, 1st July, noon) by applying a factor 4.7 to those measured in CESAM chamber (see section 2.2); [b] estimated for [OH] = 2 × 10^6 molecule cm^{-3}

574

576